

Laboratory comparison of field portable X-ray fluorescence spectrometer (FP-XRF) and inductively coupled plasma mass spectrometry (ICP-MS) for determination of airborne metals in stainless steel welding fume

Ashley Newton, Ana M. Rule, Berrin Serdar & Kirsten Koehler

To cite this article: Ashley Newton, Ana M. Rule, Berrin Serdar & Kirsten Koehler (2023) Laboratory comparison of field portable X-ray fluorescence spectrometer (FP-XRF) and inductively coupled plasma mass spectrometry (ICP-MS) for determination of airborne metals in stainless steel welding fume, Journal of Occupational and Environmental Hygiene, 20:11, 536-544, DOI: [10.1080/15459624.2023.2244022](https://doi.org/10.1080/15459624.2023.2244022)

To link to this article: <https://doi.org/10.1080/15459624.2023.2244022>



View supplementary material [↗](#)



Published online: 14 Sep 2023.



Submit your article to this journal [↗](#)



Article views: 172



View related articles [↗](#)



View Crossmark data [↗](#)



Laboratory comparison of field portable X-ray fluorescence spectrometer (FP-XRF) and inductively coupled plasma mass spectrometry (ICP-MS) for determination of airborne metals in stainless steel welding fume

Ashley Newton^a , Ana M. Rule^a , Berrin Serdar^b, and Kirsten Koehler^a 

^aEnvironmental Health and Engineering, Bloomberg School of Public Health, Johns Hopkins University, Baltimore, Maryland;

^bEnvironmental Health Associates LLC, Englewood, Colorado

ABSTRACT

Welding fume is a common exposure in occupational settings. Gravimetric analysis for total particulate matter is common; however, the cost of laboratory analyses limits the availability of quantitative exposure assessment for welding fume metal constituents in occupational settings. We investigated whether a field portable X-ray fluorescence spectrometer (FP-XRF) could provide accurate estimates of personal exposures to metals common in welding fume (chromium, copper, manganese, nickel, vanadium, and zinc). The FP-XRF requires less training and is easier to deploy in many settings than traditional wet laboratory analyses. Filters were analyzed both by FP-XRF and inductively coupled plasma mass spectrometry (ICP-MS). We estimated the FP-XRF limit of detection for each metal and developed a correction factor accounting for the non-uniform deposition pattern on filter samples collected with an Institute of Medicine (IOM) inhalable particulate matter sampler. Strong linear correlation was observed for all metals ($0.72 < r < 0.96$). The median percent bias for chromium and nickel was less than 15%. The linear slope between the two methods for some metals (copper, manganese, and zinc) was greater than 1, indicating that the FP-XRF overestimated metal mass (median percent bias for vanadium was the largest at 94%), but the linearity of the response suggests that appropriate correction factors could be developed.

KEYWORDS

Analysis methods; metals; particulate matter; welding fume



Introduction

Welding fume is produced when metals are vaporized during the welding process and condense into fumes (Jeffus 2003). These fumes are predominately composed of fine and ultrafine particles (aerodynamic equivalent diameters [d_a] less than 2.5 or 0.1 μm , respectively) and contain varying levels of particulate metals, including chromium, nickel, manganese, lead, iron, and zinc (Antonini 2014). While the metallurgical composition of the fume is dependent on many factors (e.g., composition of the base and joining metals, presence of metal coatings or fluxes, and the welding process being used), welding on stainless steel is generally known to produce high fume concentrations of nickel and chromium as compared to other methods (Jeffus 2003; Antonini 2014).

The International Agency for Research on Cancer (IARC) has classified both nickel and the hexavalent

species of chromium as Group 1 human carcinogens, and manganese is both cyto- and neurotoxic (Williams et al. 2012; IARC 2018). Occupational manganese exposure has also been associated with parkinsonian-like syndrome (Antonini 2003; Andruska and Racette 2015). Although no occupational exposure limit (OEL) has existed for welding fume in the United States since the 1989 Occupational Safety and Health Administration (OSHA) permissible exposure limit (PEL) was vacated in 1992 (NIOSH 2007), there has been a renewed interest in the health effects of welding fume since IARC reclassified it from a Group 2B to a Group 1 human carcinogen in 2017 (IARC 2018).

Although there are approximately eleven million full-time welders worldwide and an additional 110 million workers incurring incidental welding-fume exposures (Guha et al. 2017), welding fume is difficult to comprehensively assess in occupational settings.

CONTACT Kirsten Koehler  kkoehle1@jhu.edu  Environmental Health and Engineering, Bloomberg School of Public Health, Johns Hopkins University, Baltimore, Maryland.

 Supplemental data for this article can be accessed online at <https://doi.org/10.1080/15459624.2023.2244022>. AIHA and ACGIH members may also access [supplementary material](http://oeh.tandfonline.com) at <http://oeh.tandfonline.com>.

© 2023 JOEH, LLC

While gravimetric analysis for total particulate matter (PM) can be determined relatively inexpensively, element specific exposures (e.g., chromium, nickel, manganese) typically require expensive laboratory analysis (on the order of \$100 per sample) and often take several weeks or more to receive results at in-house laboratories and even longer if the analysis is performed at an outside laboratory. As such, quantitative exposure assessments to welding fume constituents are relatively rare in the literature for large cohort studies.

Traditional laboratory methods for metals analysis include inductively coupled plasma optical emission spectroscopy (ICP-OES), wavelength dispersive sequential X-ray fluorescence spectroscopy (WDXRF), or flame atomic absorption spectroscopy (flame-AAS) (Harper et al. 2007; Laohaudomchok et al. 2010; Gorce and Roff 2016). Recent studies in the literature have developed screening methods for several metals in occupational air filter samples using field-portable X-ray fluorescence spectrometers (FP-XRF) as opposed to these more expensive laboratory methods. The US National Institute for Occupational Safety and Health (NIOSH) has also published a standardized method for the use of FP-XRF in screening for airborne lead (NIOSH 1998). In comparison to wet-lab chemical methods, FP-XRF requires little sample preparation and less training for laboratory or study personnel, allows for analysis of the filter at the site of collection, and typically completes analysis in less than five minutes per filter. Additionally, XRF analysis is nondestructive, allowing for subsequent chemical analyses. However, the FP-XRF also has higher metal-specific limits of detection than most traditional laboratory methods, especially for lower atomic number elements like chromium. Additionally, the instrument precision can vary with respect to the element mass concentration (Lawryk et al. 2009).

Institute of Medicine (IOM) samplers (SKC Inc, Eighty Four, PA) are a common and commercially available occupational sampler to measure the inhalable size fraction ($d_a < 100 \mu\text{m}$) of PM. However, IOM filters pose a challenge for XRF analyses because they are not loaded homogeneously across the filter surface and exhibit a characteristic grid-like pattern of particle deposition. As most commercially available FP-XRF instruments only analyze a small cross section of the total filter area, heterogeneous loadings could bias the observed result depending on the fraction of the measured filter surface with and without deposited PM present.

To evaluate the accuracy and precision of FP-XRF in determining the mass concentration of chromium, copper, manganese, nickel, vanadium, and zinc on non-homogeneously loaded filters, inhalable metal exposures were measured with IOM samplers in a cohort of stainless steel welders. Samples were analyzed with FP-XRF and inductively coupled plasma mass spectrometry (ICP-MS). Image analysis of an exemplar IOM deposition pattern was evaluated and used to produce a correction factor accounting for non-homogeneous loading of the filter surface.

Methods

Study population

The study population was recruited from a stainless steel manufacturing facility near Boise, Idaho in October and November of 2017. Eighteen workers employed either as full-time welder/fabricators or laser operators were recruited to participate. All participants were administered informed consent and the the Colorado Multiple Institutional Review Board (COMIRB) approved this study (#15-1699).

Eighteen participants were monitored for exposure to inhalable PM and inhalable metals for the duration of their work shift on 2 days over a 1-month study period for a total of 36 monitored shifts (one participant had a single measurement, while another had three samples). Post-shift surveys were administered to collect work history information and time-task logs for all welding and grinding/cutting performed that day. Fourteen of the 18 participants reported welding professionally at least half-time for more than 3 years (mean = 10.9; IQR = 2.75–13.5 years), with three participants having welded for less than a year. Approximately 85% of welding hours recorded by the participants were for Gas Tungsten Arc Welding (GTAW) on stainless steel, and most remaining hours were attributed to Gas Metal Arc Welding on mild steel.

Air sampling

Study participants wore an Institute of Medicine (IOM) inhalable sampler at the center of their collar, just below the bottom of the welding hood (Newton et al. 2021). IOM cassettes were measured gravimetrically for inhalable PM and the filters were analyzed via both FP-XRF and ICP-MS for metals analysis.

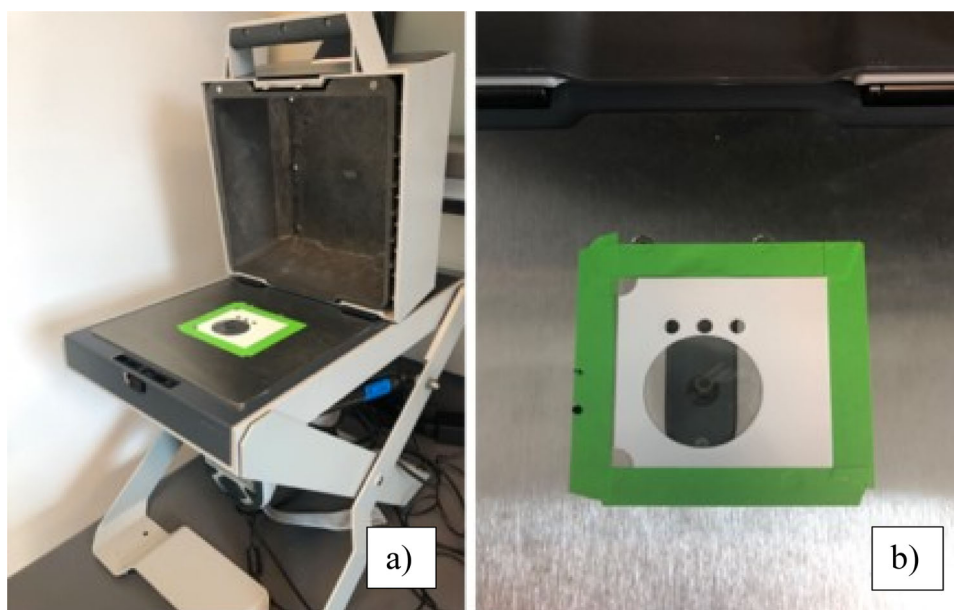


Figure 1. (a) Filter holder placed over FP-XRF analysis stand and (b) filter holder.

Gravimetric analysis

The 36 IOM filters and cassettes used in this study were pre- and post-weighed in a temperature and humidity-controlled weighing room at Johns Hopkins School of Public Health using a Mettler Toledo microbalance (Columbus, OH; ± 0.001 mg). Given that particles are known to deposit on the IOM sampler walls, standardized methods for determining the inhalable mass concentration require weighing the filter in combination with the cassette as opposed to the filter alone (HSE Method MDHS 14/4, 2014). However, as only the filter was analyzed for metals using the FP-XRF, pre- and post-weights were also measured for the filter alone in order to compare filter loading more accurately to metal content. Filters were only handled using Teflon-coated forceps.

Chemicals and materials

All chemicals were analytical grade or higher and used as received without further purification. Single and multi-element standards were purchased from Inorganic Ventures (Christiansburg, VA) and a certified reference material (CRM) for stainless steel welding fume (SSWF-1 CRM) was from Health and Safety Laboratory (Harpur Hill, Buxton, UK). Concentrated nitric and hydrofluoric acid (TraceMetal grade) were purchased from Fisher Scientific (Waltham, MA) and hydrogen peroxide (Suprapur grade) was purchased from Millipore Sigma (Burlington, MA). IOM samplers and mixed cellulose ester (MCE) filters (25 mm,

0.8 μ m pore size) were purchased from SKC Inc. (Eighty Four, PA).

Field portable XRF analysis

Analysis for elemental components on all filters was conducted using a NITON Portable XRF model XL3t series 600 (Thermo Fisher Scientific, Waltham, MA) mounted in the associated test stand (Figure 1(a)). A single layer of X-ray transparent Mylar film from an XRF filter holder (Thermo Scientific, Waltham, MA) was centered over the analysis window of the FP-XRF stand (Figure 1(b)). The Mylar film prevents the filter from directly touching either the instrument or the stand surface, thus limiting potential cross-contamination of samples or instrumentation. The 25 mm IOM filters were placed on the Mylar film for analysis so that the 8 mm X-ray beam diameter would pass through approximately the center of the filter (Figure 2(a)). Using the “Standard Thin Film” setting, all readings were set for 90 s of exposure time per element group (low Z group, main group, and high Z group) for a total analysis time of 270 s per filter. As measurement of the X-ray emissions occurs continuously during the time when the sample is exposed to the excitation source, increasing the exposure time generally increases the precision and accuracy of the reading. The FP-XRF software allows for the exposure time to range from 30 s to 120 s. All filters were measured in triplicate from the centered position and the Mylar film was replaced between filters to prevent contamination. Each time the FP-XRF was turned on

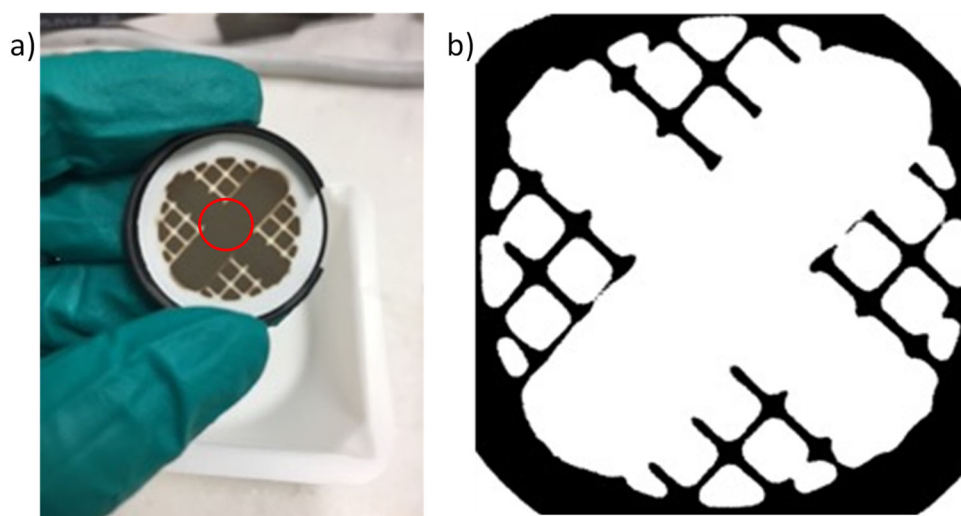


Figure 2. (a) Example of typical IOM deposition pattern. Red circle indicates approximate position and scale of analysis window. (b) Processed, binary image of filter where each pixel with deposited PM was converted to white and each pixel without deposited PM was converted to black using ImageJ software.

for analysis, a system check was performed. Additionally, at the beginning and end of each day the FP-XRF was used we completed a verification of a commercially prepared calibration standard to ensure Cr, Ni, and Mn measurements were within manufacturer error limits and a blank filter (filter directly from the package) was analyzed to ensure there were no indications of system contamination.

Chromium and vanadium were measured using the Low Z group mode and manganese, nickel, copper, and zinc were measured in the main group mode. Cadmium was measured in the high Z mode, but all results were below method limits of detection (LOD) for both FP-XRF and ICP-MS and are not presented here.

The FP-XRF's Fundamental Parameter analysis software directly provides measurements in $\mu\text{g}/\text{cm}^2$ for all tested elements but does not typically allow for direct quantitative determination of instrument LODs. The manufacturer reported LOD is for analysis of bulk soil samples, and not directly applicable to thin films. For low masses, the FP-XRF only indicates that the value was below the method LOD but does not provide a numeric value. For blank filters, all measurements were below the method LOD. As such, we were unable to estimate the LOD from the standard deviation of the estimated masses of the blank filters. Instead, for each element, we estimated the LOD from the three filters with the lowest mass per square centimeter in which all three replicate measurements were reportable. The mean value across the three replicate measurements was subtracted from the individual values for each filter and the LOD was defined as three

times the standard deviation of the mean-subtracted values. Since we wish to do a pairwise comparison of values between the FP-XRF and the ICP-MS, any values reported either as undetected or below the element specific LOD were substituted by the $\text{LOD}/\sqrt{2}$ (Hornung and Reed 1990; Croghan and Egeghy 2003; Hewett and Ganser 2007).

Calculation of FP-XRF filter mass

The mass deposition pattern of an IOM filter with a typical particulate loading for this cohort was analyzed using ImageJ (US National Institutes of Health Bethesda, MD). A photograph of one loaded filter (Figure 2) was processed such that each pixel showing deposited PM was converted to white and each pixel without deposited PM was converted to black. Thresholds determining if each pixel represented an area with deposition or without deposition were based on the coloration differences between deposited PM and blank filter and were derived using ImageJ's 'Make Binary' command. The binary image was then analyzed to estimate the loading correction factor, which was the fraction of white pixels compared to total pixels for the filter. Multiplying the loading correction factor by the total filter surface area provided an estimate of the total filter surface area with detectable PM loading.

In order to compare FP-XRF measurements to those from the ICP-MS, the measured FP-XRF mass per surface area ($\mu\text{g}/\text{cm}^2$) measured in the center of the filter (an area with PM deposition) was multiplied by the total filter surface area and multiplied by the

loading correction factor to produce mass per filter ($\mu\text{g}/\text{filter}$). It was assumed that there was equal loading on all portions of the filter with PM deposition.

ICP-MS analysis

All filters were prepared for ICP-MS analysis using a strong acid microwave-assisted digestion method. Additionally, PM deposited on the sides of the IOM inlet was collected by wiping with $2\text{ cm} \times 2\text{ cm}$ squares of KimWipe (Thomas Scientific, Swedesboro, NJ). IOM filters and IOM inlet wipes were placed in separate 50 mL Teflon microwave vessels with 4 mL 70% HNO_3 , 2 mL 35% H_2O_2 , and 0.35 mL 49% HF. The samples were then sealed and digested in a Mars 5 Xpress scientific microwave (CEM Corporation, Matthews, NC) using a 17-minute three-stage temperature-controlled program. The final temperature of 180°C was held for five minutes with intermediate two-minute ramps and three-minute holds at 95°C and 135°C .

Digested samples were then diluted and analyzed using an Agilent 7500 Series Octopole ICP-MS (Agilent Technologies, Santa Clara, CA). Percent recovery for chromium, manganese, and nickel was verified as $95 \pm 5\%$ using the stainless steel welding fume CRM (Health and Safety Laboratory, Harpur Hill, Buxton, UK). Certified values for zinc, copper, and vanadium were not provided for this CRM and thus percent recoveries for those elements could not be calculated. Blanks, spikes, and duplicates were carried out at a rate of one in every 10 samples. Spikes were generated by preparing known concentrations of a matrix-matched multi-elemental standard. Duplicates were prepared by taking repeat aliquots of concentrated digestants and diluting prior to analysis.

Statistical analysis

Spearman correlation coefficients were calculated to determine the correlation between the FP-XRF and ICP-MS measurements for each metal and Wilcoxon matched-pairs signed-rank tests were used to test for equality of the median between FP-XRF and ICP-MS observations. Linear regressions between FP-XRF and ICP-MS were also computed and are displayed graphically on scatter plots comparing the two measurement methods. Bland-Altman plots were used to assess whether accuracy or precision varied by filter loading.

Results from the triplicate FP-XRF analysis of the filters were used to determine relative standard

deviations (RSD) as a measure of instrument precision. The RSD was calculated by dividing the standard deviation of the filter triplicate readings by the filter mean for filters in which at least two of the FP-XRF measurements were above the estimated LOD. The median and range of observed RSDs are reported.

All statistical analyses were performed using Stata 14 (StataCorp, College Station, TX) and Matlab 2022a (MathWorks, Natick, MA).

Results

Filter gravimetric and visual analysis

A total of 36 IOM filters were analyzed in this study. One sample only ran for 35 min and was excluded from further analyses leaving an analytical sample size of 35 filters. The mean inhalable gravimetric mass concentration, including mass from sampler wall deposits, was 2.05 (range: $0.31\text{--}5.17$) mg/m^3 (Newton et al. 2021). The ImageJ analysis indicated that deposited PM was detectable on approximately 69% of the total IOM filter surface, making the loading correction factor 0.69. This value was used to calculate the FP-XRF filter mass in all subsequent analyses.

FP-XRF measurements

The median and range of elemental mass per filter is reported in Table 1, where values below the LOD have been replaced by $\text{LOD}/\sqrt{2}$ for all 35 samples. The median mass per filter, accounting for the loading correction factor, was 43, 4.9, 23, 20, 0.33, and 5.1, μg for chromium, copper, manganese, nickel, vanadium, and zinc, respectively. The estimated LOD ranged from 0.09 to $0.60\text{ }\mu\text{g}/\text{cm}^2$ for these six metals (Table 1). The number of filters with at least two readings above the estimated LOD and the median and range of the RSD deviation between the replicate measurements for these filters are also displayed in Table 1. Briefly, 100% filters had FP-XRF detectable mass concentrations for chromium, whereas only 34% of filters had at least two out of three detectable measurements for Vanadium. With the exception of vanadium ($\text{RSD} = 20\%$), the median RSD was below ten percent for the other five metals.

Comparison between FP-XRF and ICP-MS measurements

The median (range) elemental mass per filter from the ICP-MS analyses are shown in Table 1. Comparisons of ICP-MS and FP-XRF elemental mass per filter

Table 1. Median and range of ICP-MS and FP-XRF filter elemental mass concentrations ($N = 35$).

	ICP-MS		FP-XRF			Method comparison
	Filter mass median (range) [μg]	Filter mass* median (range) [μg]	Estimated LOD [$\mu\text{g}/\text{cm}^2$]	Sample size above LOD	RSD median (range) [%]	% bias median (range) [%]
Chromium	42 (9.3–241)	43 (5.8–200)	0.20	35	2 (1–13)	9.9 (–86.3 – 52.6)
Copper	3.2 (0.4–22)	4.9 (0.6–14)	0.16	30	7 (3–65)	44.0 (–76.0 – 196.1)
Manganese	16 (1.3–113)	23 (0.7–157)	0.24	32	6 (1–25)	39.4 (–57.1 – 59.2)
Nickel	19 (3.9–107)	21 (1.8–91)	0.60	34	4 (0–28)	13.2 (–87.5 – 54.8)
Vanadium	0.2 (0.04–1.2)	0.3 (0.2–1.1)	0.09	12	20 (6–47)	97.4 (–31.2 – 467.3)
Zinc	3.8 (0.7–260)	5.2 (0.9–611)	0.39	26	4 (1–27)	43.2 (–52.3 – 150.7)

Notes. Estimated LOD, sample size above the LOD (number of samples with at least two measurements above the limit of detection by the FP-XRF) and the average relative standard deviation among the detectable samples are shown for the FP-XRF. The last column shows the median and range of percent differences between the FP-XRF and ICP-MS for all 35 samples.

*Values below the LOD were replaced by $\text{LOD}/\sqrt{2}$.

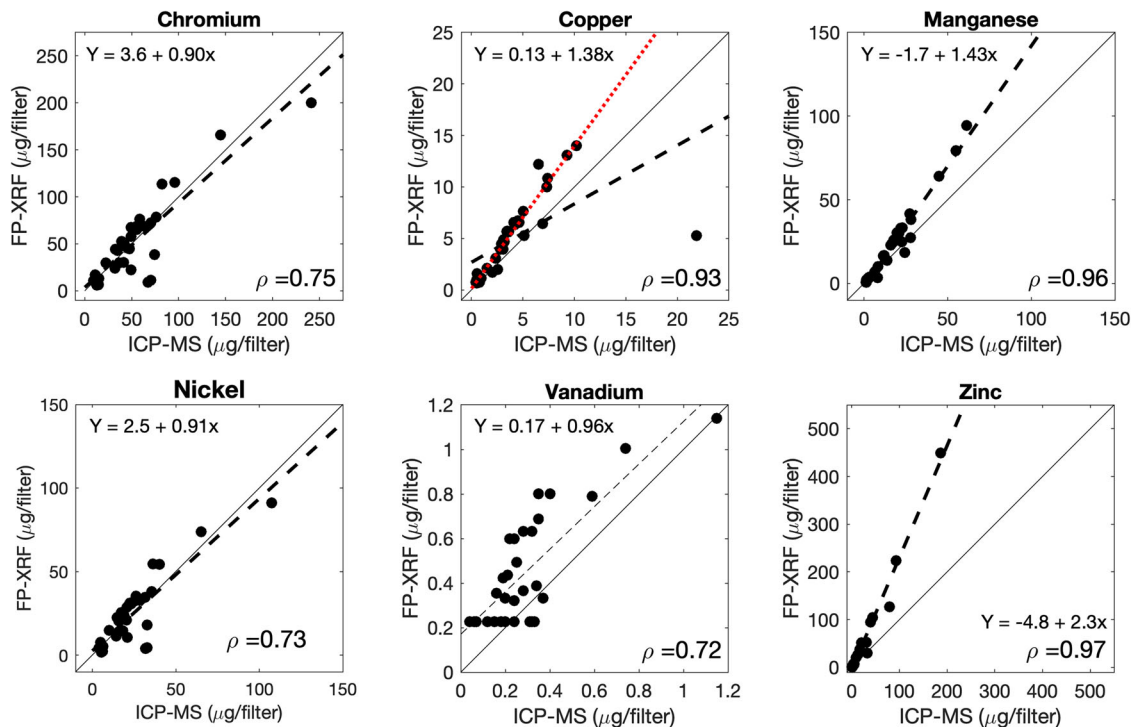


Figure 3. Comparison of elemental filter mass from ICP-MS (filter only) and FP-XRF (filter only). the linear fit to the data is shown in the dashed line and the linear equation is included in the inset. The Spearman correlation coefficient (ρ) is also listed. The solid line is the 1:1 reference line. For copper, the red dotted line shows the linear fit with the outlier removed (the linear equation is shown for this line only; the correlation coefficient is for all data).

measurements are shown in Figure 3. Regression lines were fitted for each element (dashed lines) and the 1:1 line is shown for reference. For the six metals of interest measurements were highly correlated between the two methods ($\rho \geq 0.72$). For chromium and nickel, the linear regression intercepts were near zero (compared to the range of the data) and the slopes were close to 1 (0.90 for chromium and 0.91 for nickel). However, for manganese, copper, and zinc the FP-XRF readings

were generally higher than those observed using ICP-MS, with slopes of the linear regressions ranging from 1.38 to 2.3. Vanadium concentrations also tended to be overestimated. For this metal, the slope of the linear regression was close to 1, but the intercept was greater than zero, resulting in this overestimation. Median percent bias was positive for all metals ranging from about 10% for chromium to 97% for vanadium. For copper, an extreme outlier was present and a linear fit without

the inclusion of this outlier is shown in the red dotted line (the linear equation corresponds to this line). The correlation coefficient using all data was 0.93 and increased to 0.96 excluding the outlier. All Spearman correlation coefficients for all metals were statistically significant ($p < 0.001$).

A Wilcoxon signed-rank test showed a statistically significant equivalence in population medians between the nickel and chromium concentrations measured using ICP-MS and FP-XRF (Nickel: $p = 0.19$; Cr: $p = 0.44$ indicates test fails to reject the null hypothesis that the difference between the ICP-MS and FP-XRF has a zero median); no other element showed a statistically significant inter-method equality. Bland-Altman plots for the ICP-MS and FP-XRF measurements are shown in Figure 4. The solid lines represent the mean of the absolute value of the measurement difference (FP-XRF minus ICP-MS) and the dashed lines represent the 95% limits of accuracy (LoA). While method differences for chromium and nickel appear to cluster mostly randomly around the mean, there are clear trends evident for zinc and manganese, in particular. As element-specific filter loading increases, the FP-XRF increasingly overestimates the ICP-MS observed mass for these two metals, a trend which can also be seen in the correlation plots in Figure 3.

Considerations for the IOM sampler

The IOM sampler can have substantial PM deposition on the sampler walls. As the FP-XRF method only measured filter mass loadings from the IOM filter and did not account for any PM deposited on the walls of the sampler, the FP-XRF method is expected to be biased low when using it with the IOM sampler or any other sampler that necessitates measuring particle deposition on sampler walls. Since the FP-XRF requires that analyzing a small area of the sample can provide a reasonable estimate of loading over the entire sampled surface, it is unlikely the wipe samples could provide reasonable estimates of the wall deposited mass. For chromium and nickel, the two elements that showed statistically significant equivalence in population medians, Bland Altman plots indicating the total difference in mass and the percent difference in mass when comparing the total ICP-MS observed mass (filter plus wall deposits) and FP-XRF observed mass (filter only) are shown in the Online Supplement (Figure S1). The mean difference between the two methods went from -1.5 to -9.3 for chromium and from 0.5 to -3.6 for nickel. Since the FP-XRF was found to overestimate concentrations for the other four metals, comparison between the FP-XRF (filter only) and inhalable ICP-MS (filter plus

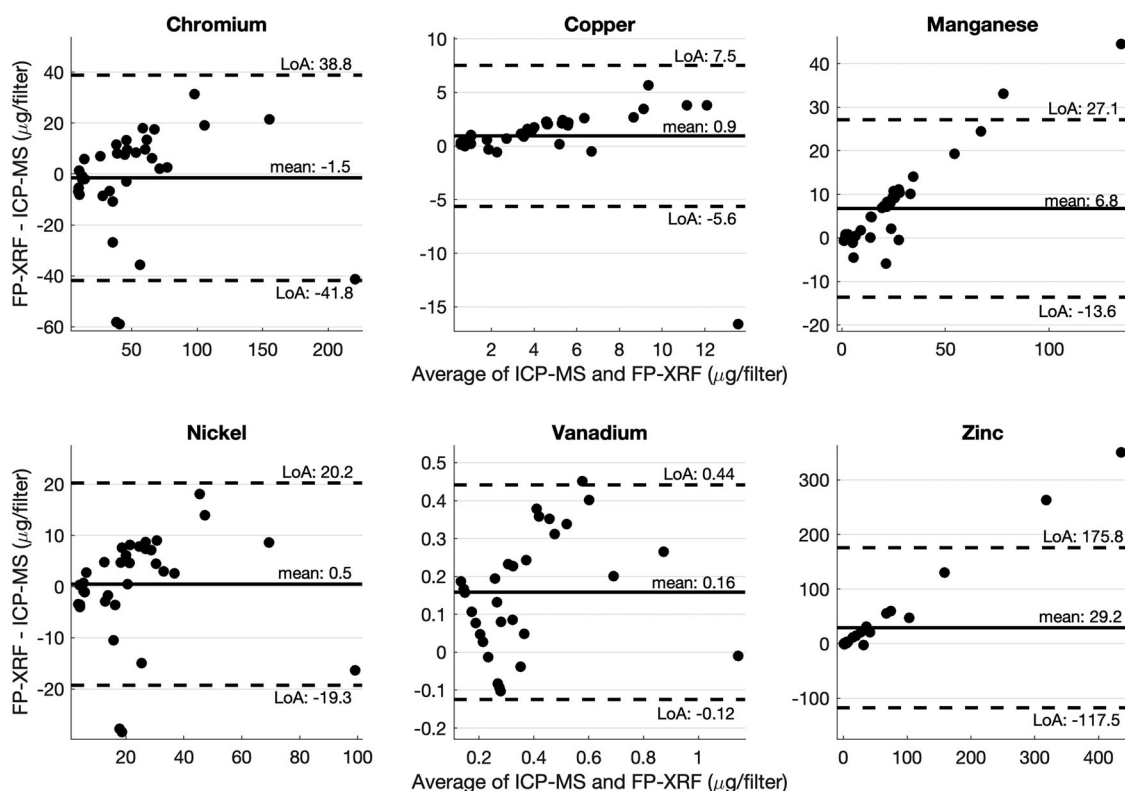


Figure 4. Bland-Altman plots for ICP-MS (filter only) and FP-XRF (filter only) measurements. Solid lines represent the mean value of the FP-XRF method minus the ICP-MS method. The 95% limits of accuracy (LoA) are shown as dashed lines.

wipe) was not completed as it could suggest improvement in the accuracy that is spurious.

Discussion

The observed masses measured by the FP-XRF tended to be higher than those measured by the ICP-MS, particularly for copper, manganese, vanadium, and zinc. The trend for positive bias of FP-XRF readings when comparing to reference methods is also evident in other studies in the literature (Harper et al. 2007; Laohaudomchok et al. 2010; Gorce and Roff 2016). In comparing FP-XRF derived measurements to ICP-OES, for example, Harper et al. found XRF analyses were on average 850% higher than ICP-OES for chromium, 20% higher for nickel, and 60% higher for manganese across different industrial environments. The extreme difference in chromium is suggestive of incomplete digestion of the filters prior to ICP-OES analysis in that study. In comparison, the digestion method used in our study was verified to have $95\% \pm 5\%$ recovery for chromium, manganese, and nickel using a CRM for stainless steel welding fume. While our median percent bias for chromium of $\sim 10\%$ is significantly lower than Harper et al. the magnitudes of bias in this study for nickel and manganese, 13% and 39%, respectively, are similar. Given the large variations in welding fume's physicochemical characterization as a result of the welding process and other metallurgical considerations, incomplete digestion of the welding fume may still be possible in our samples if it contained a higher amount of spinels, or other difficult to digest metal oxide formations, than the welding fume used to create the CRM (Hewitt and Madden 1986).

Triplicate FP-XRF measurements on the central portion of an IOM filter showed good precision between readings, with relative standard deviations below 10% for all metals except vanadium, which had a much smaller detectable sample size (at least two of three readings above the LOD) than the other metals (12 vs. at least 26). Strong linear correlations were observed between FP-XRF and ICP-MS measurements of the IOM filters for all metals. These correlations are very similar in magnitude to a recent study comparing FP-XRF to laboratory XRF (WDXRF) for manganese ($\rho = 0.96$ ICP-MS; $\rho = 0.995$ WDXRF), copper ($\rho = 0.96$ ICP-MS; $\rho = 0.97$ WDXRF), and zinc ($\rho = 0.97$ ICP-MS; $\rho = 0.936$ WDXRF), although the sample sizes were larger in the study comparing the field portable to the laboratory XRF (Laohaudomchok et al. 2010). We observed a higher correlation between methods for chromium ($\rho = 0.75$ ICP-MS; $\rho = 0.33$ WDXRF), which may be a result of higher

masses present on the filters in our study (Laohaudomchok et al. 2010).

Another possible explanation for the trend of FP-XRF overestimation of manganese at higher mass loadings is spectral interference. Chromium and iron both absorb the same wavelength as emissions from the K_{α} orbital of manganese (Lawryk et al. 2009). As manganese, iron, and chromium are all welding-associated elements, it is reasonable to assume that as manganese levels increase, so too do iron and chromium. The FP-XRF software is designed to account for these interferences, but the adjustment may not be sufficient at high mass levels. Additionally, tungsten levels may interfere with zinc, but area tungsten levels reported from the study site do not appear to be high enough to account for the level of difference observed (mean area mass concentrations of PM_{10} tungsten were $0.25 \mu\text{g}/\text{m}^3$ or smaller) (Newton et al. 2021).

The FP-XRF method will lead to bias for samplers that include particle deposition on sampler walls. Wall losses are typically reported as less than 30% of the total sample in the literature (Harper et al. 2007), consistent with that found in this study (mean percent difference for nickel and chromium between the filter and the inhalable mass [filter plus wall wipe] was -14%). However, size distribution of the particles and their chemical composition may be heterogenous between the filter and wall deposition. The overestimation of the FP-XRF for some metals could result in better agreement with the inhalable mass (accounting for wall mass) for some metals that are spurious.

Limitations

A limitation in this study is the relatively small sample size with only 35 filters used for this comparison from a single facility. Also, the CRM used to determine elemental percent recovery did not provide certified values for copper, zinc, or vanadium and thus the strength of the digestion process could not be judged for those elements. Additionally, only one correction factor for non-homogenous filter loadings was calculated using the pixel-threshold process. In future studies, this should be performed for each filter (or among a group of filters to determine variability on filter loading) as different mass loadings may alter the percent of filter with detectable deposition.

Conclusion

Corrected FP-XRF elemental mass concentrations for IOM filters are strongly linearly correlated with

ICP-MS measurements for six metals. Overall, mass concentrations determined by the FP-XRF show a positive bias compared to the ICP-MS, but the linear relationship suggests that appropriate calibration factors could be developed through future work.

Ethical approval

For this study, all participants were administered informed consent and the Colorado Multiple Institutional Review Board (COMIRB) approved this study (#15-1699).

Disclosure statement

No potential conflict of interest was reported by the author(s).

Funding

This research was funded under support from the Johns Hopkins University Education and Research Center for Occupational Safety and Health (ERC). ERC training grant funding comes from the National Institute for Occupational Safety and Health (NIOSH), under Grant No. 5 T42 OH 008428. This project was also funded through NIOSH under Grant No. R21 OH 010661.

ORCID

Ashley Newton  <http://orcid.org/0000-0001-6717-0096>
Ana M. Rule  <http://orcid.org/0000-0003-2328-0749>
Kirsten Koehler  <http://orcid.org/0000-0002-0516-6945>

Data availability statement

The data that support the findings of this study are available from the corresponding author upon reasonable request.

References

- Andruska KM, Racette AB. 2015. Neuromyothology of man-ganism. *Curr Epidemiol Rep.* 2(2):143–148. doi:10.1007/s40471-015-0040-x.
- Antonini JM. 2003. Health effects of welding. *Crit Rev Toxicol.* 33(1):61–103. doi:10.1080/713611032.
- Antonini JM. 2014. Health effects associated with welding. In: Hashmi S, Ferreira Batalha G, Yilbas B, editors. *Comprehensive materials processing*. Amsterdam: Elsevier Ltd. p. 40–79.
- Croghan CW, Egeghy P. 2003. Methods of dealing with val-ues below the limit of detection using SAS. *South SAS User Group.* 22(24):22–24.
- Gorce JP, Roff M. 2016. Immediate screening of lead expos-ure in the workplace using portable X-ray fluorescence. *J Occup Environ Hyg.* 13(2):102–111. English. doi: 10.1080/15459624.2015.1091959.
- Guha N, Loomis D, Guyton KZ, Grosse Y, El Ghissassi F, Bouvard V, Benbrahim-Tallaa L, Vilahur N, Muller K, Straif K. 2017. Carcinogenicity of welding, molybdenum trioxide, and indium tin oxide. *Lancet Oncol.* 18(5): 581–582. eng. doi:10.1016/S1470-2045(17)30255-3.
- Harper M, Pacolay B, Hintz P, Bartley DL, Slaven JE, Andrew ME. 2007. Portable XRF analysis of occupational air filter samples from different workplaces using differ-ent samplers: final results, summary and conclusions. *J Environ Monit.* 9(11):1263–1270. eng. doi:10.1039/b710591f.
- Hewett P, Ganser GH. 2007. A comparison of several meth-ods for analyzing censored data. *Ann Occup Hyg.* 51(7): 611–632. English. doi:10.1093/annhyg/mem045.
- Hewitt PJ, Madden MG. 1986. Welding process parameters and hexavalent chromium in MIG fume. *Ann Occup Hyg.* 30(4):427–434.
- Hornung RW, Reed LD. 1990. Estimation of average con-centration in the presence of nondetectable values. *Appl Occup Environ Hyg.* 5(1):46–51. doi:10.1080/1047322X.1990.10389587.
- International Agency for Research on Cancer (IARC). 2018. Welding, molybdenum trioxide, and indium tin oxide. In: International Agency for Research on Cancer, editor. *IARC monographs on the evaluation of carcinogenic risks to humans*. Lyon (France): International Agency for Research on Cancer.
- Jeffus L. 2003. *Welding: principles and applications*. 5th ed. Clifton Park (NY): Delmar Learning.
- Laohaudomchok W, Cavallari JM, Fang SC, Lin X, Herrick RF, Christiani DC, Weisskopf MG. 2010. Assessment of occupational exposure to manganese and other metals in welding fumes by portable X-ray fluorescence spectrom-eter. *J Occup Environ Hyg.* 7(8):456–465. eng. doi: 10.1080/15459624.2010.485262.
- Lawryk NJ, Feng HA, Chen BT. 2009. Laboratory evaluation of a field-portable sealed source X-ray fluorescence spec-trometer for determination of metals in air filter samples. *J Occup Environ Hyg.* 6(7):433–445. eng. doi:10.1080/15459620902932119.
- National Institute for Occupational Safety and Health (NIOSH). 1998. *Lead by field portable XRF*. NIOSH manual of analytical methods. Cincinnati (OH): National Institute for Occupational Safety and Health.
- National Institute for Occupational Safety and Health (NIOSH). 2007. Appendix G: 1989 air contaminants update project – exposure limits not in effect. NIOSH pocket guide to chemical hazards. Pittsburgh (PA): Department of Health and Human Services; p. 424a.
- Newton A, Adams K, Serdar B, Dickinson LM, Koehler K. 2021. Personal and area exposure assessment at a stain-less steel fabrication facility: an evaluation of inhalable, time-resolved PM(10,) and bioavailable airborne metals. *J Occup Environ Hyg.* 18(2):90–100. eng. doi:10.1080/15459624.2020.1854460.
- Williams M, Todd GD, Roney N, Crawford J, Coles C, McClure PR, Garey JD, Zaccaria K, Citra M. 2012. Agency for toxic substances and disease registry (ATSDR) toxicological profiles. Toxicological profile for manganese. Atlanta (GA): Agency for Toxic Substances and Disease Registry (US).